Rotational bands in open antiferromagnetic rings: A neutron spectroscopy study of Cr_8Zn

A. Bianchi, S. Carretta, P. Santini, and G. Amoretti
Dipartimento di Fisica, Università di Parma, I-43100 Parma, Italy and S3-CNR-INFM, I-41100 Modena, Italy

T. Guidi
ISIS Pulsed Neutron Facility, Rutherford Appleton Laboratory, Chilton OX11 0QX, United Kingdom

Y. Qiu
Department of Materials Science and Engineering, University of Maryland, College Park, Maryland 20742, USA and NIST Center for Neutron Research, National Institute of Standards and Technology, Gaithersburg, Maryland 20899, USA

J. R. D. Copley
NIST Center for Neutron Research, National Institute of Standards and Technology, Gaithersburg, Maryland 20899, USA

G. Timco, C. Muryn, and R. E. P. Winpenny
Department of Chemistry, University of Manchester, Manchester M13 9PL, United Kingdom
(Received 29 December 2008; published 16 April 2009)

Low-lying excitations in closed antiferromagnetic rings can be described in terms of rotational bands, which reflect the peculiar internal spin structure of the corresponding eigenstates. Here we use inelastic neutron-scattering measurements on the Cr_8Zn molecule to investigate the validity of the rotational band picture in magnetically open rings. We determine the parameters of the microscopic spin Hamiltonian describing each Cr_8Zn molecule and we analyze how the spin dynamics changes with respect to the parent closed-ring compound Cr_8. Qualitative differences can be found not only in the energy-level diagrams but also in the internal structure of the spin eigenstates, probed through the wave-vector transfer dependence of the neutron cross section. The usual rotational bands picture fails because quantum fluctuations of the total-spin length of the two sublattices do not occur jointly due to the ring opening.

DOI: 10.1103/PhysRevB.79.144422 PACS number(s): 75.50.Xx, 78.70.Nx, 75.10.Jm, 75.40.Gb

I. INTRODUCTION

Nanosize magnetic clusters are composed of a magnetic core of several transition-metal ions surrounded by organic ligands, which provide superexchange paths for intramolecular interactions between magnetic centers, and prevent intermolecular ones. Thus, bulk measurements reflect the properties of individual molecules since these can be regarded as isolated magnetic entities. Different technological applications in the field of information storage, quantum computation, and magnetorefrigeration have been envisaged.[1–3] In addition, magnetic molecules are ideal model systems to investigate fundamental quantum phenomena.[1] A great variety of magnetic clusters have been synthesized in recent years. Of particular interest both for fundamental physics and for technological applications are antiferromagnetic (AF) ring-shaped clusters, formed by a set of N transition-metal ions arranged in an almost cyclic planar structure.[1,4–6] The possibility to chemically substitute metal ions in the cyclic structure allows to control microscopic exchange interactions and, as a consequence, the energy and spin-wave functions of the low-lying states.[7] The Cr_8Zn cluster was derived by inserting a nonmagnetic Zn^{2+} ion in the ring-shaped structure of the well-known Cr_8 compound (see Fig. 1). This lowers the ideal ring symmetry by preventing exchange interaction between two of the spins. As a result, the Cr_8Zn molecule can be regarded as a finite spin segment and thus a model system for investigating magnetic properties and finite-size effects in the one-dimensional AF Heisenberg model.

Even-membered homonuclear closed AF rings present common features in the energy spectrum: due to the compensation of the N spins they have a singlet $S=0$ ground state, whereas low-lying excited levels are arranged into rotational bands, with the lowest one (the L band) approximately following the so-called Landé rule $E(S)=2JS(S+1)/N$ with J the exchange constant and S the total spin of the state.[1,8,9] If an external magnetic field $\mathbf{H}$ is applied to the molecule, the spin ground state will sequentially change from $S=0$ to $S=1,2,3,\ldots$ as $\mathbf{H}$ increases, but each of these states will always belong to the L band. The second set of levels belongs to the so-called E bands, which are also parabolic with re-

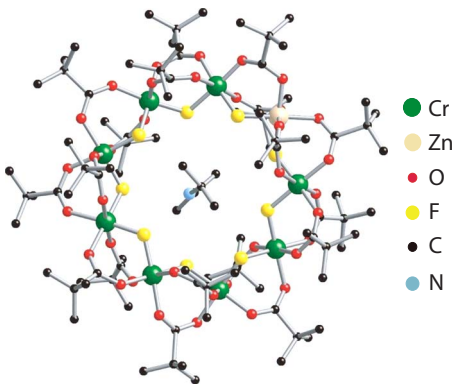

FIG. 1. (Color online) The structure of a Cr_8Zn molecule. Hydrogen atoms have been omitted for clarity.

spect to S but shifted to higher energies. In closed homometallic rings, states can be classified according to the quantum number $k=2\pi j/N$ $(j=0,\ldots,N-1)$ of the cyclic shift operator T, whose eigenvalues are e^{ik}. While the L-band states have wave vector $k=0$ or $k=\pi$, for E-band states $k=2\pi j/N$ with $j\neq 0,\ N/2$. The concept of rotational band has also been exploited to rationalize the low-temperature behavior of the complex Fe_{30} molecule, where three sublattices can be identified in its icosidodecahedron structure.[10–12]

The energies of L-band states in the opened Cr_8 ring have been investigated by macroscopic measurements on Cr_8Cd.[13,14] Magnetization and heat-capacity measurements showed deviations from the Landé rule, with a resulting different set of level crossing fields.[14] While these measurements provided information on the energy of the lowest (Landé) rotational band, the internal structure of eigenstates could not be directly probed. In addition, the higher-energy E-band states could not be directly accessed. In this paper, we exploit inelastic neutron scattering (INS) to probe the lowest-lying eigenstates of Cr_8Zn and we quantitatively analyze how the opening of the ring changes the structure of these eigenfunctions with respect to the closed version of the ring. In particular, we experimentally and theoretically show how the occurrence of disjoint quantum fluctuations of the total-spin length of the two sublattices removes the sharp separation of the low-lying states in two distinct rotational bands.

II. BASIC THEORETICAL ASPECTS

The microscopic picture of the heteronuclear open-ring Cr_8Zn is based on the following spin Hamiltonian:

$$H = J\sum_{i=1}^{7}\mathbf{s}(i)\cdot\mathbf{s}(i+1) + \sum_{i=1}^{8} d_i[s_z^2(i) - s_i(s_i+1)/3] + \sum_{i>j} D_{ij}[2s_z(i)s_z(j) - s_x(i)s_x(j) - s_y(i)s_y(j)] + \sum_{i=1}^{8} e_i[s_x^2(i) - s_y^2(i)] - \mu_B\sum_{i=1}^{8} g_i\mathbf{H}\cdot\mathbf{s}(i), \quad (1)$$

where $\mathbf{s}(i)$ is the spin operator of the ith Cr ion in the molecule $[s(i)=3/2$ for $Cr^{3+}]$. In the following we assume that the Zn^{2+} ion is in site $i=9$. In the first term of the above equation, J represents the strength of the isotropic Heisenberg nearest-neighbor exchange interaction. The second and third terms describe the axial anisotropic interactions (with the z axis perpendicular to the plane of the ring), i.e., local crystal fields (CFs) and the axial part of the dipolar interaction. D_{ij} is calculated in the point-dipole approximation. The fourth term accounts for small nonaxial anisotropy. While the actual local CFs may be much more complex than assumed in Eq. (1), experimental data are nowhere near sufficient to fix more than two CF parameters. The last term represents the Zeeman coupling with an external field $\mathbf{H}$. We use the expression given in Ref. 7 in order to simulate the powder neutron-scattering data.

Since isotropic exchange (H_{iso}) is the dominant interaction in Eq. (1), the energy spectrum is composed of total-spin multiplets split by local crystal fields. The mixing between different spin multiplets due to anisotropic interactions (S mixing) is small and does not affect the following discussion. As mentioned above, it is well-known that in closed bipartite AF rings the lowest-lying multiplets are arranged in two bands (L and E) which can be approximately described by the effective-rotor Hamiltonian

$$H_{rot} = J'\mathbf{S}_{odd}\cdot\mathbf{S}_{even} \quad (2)$$

with $\mathbf{S}_{odd,even}$ the total spin of the two sublattices, $J'=\frac{4J}{N}$, and N the number of sites. The eigenvectors of Eq. (2) have the form $|\alpha S_{odd}S_{even}SM\rangle$, where α denotes additional quantum numbers specifying the internal structure of each sublattice. The corresponding eigenvalues are $2J[S(S+1)-S_{odd}(S_{odd}+1)-S_{even}(S_{even}+1)]/N$. L-band multiplets are nondegenerate, have $k=0$ or $k=\pi$, and correspond to $S_{odd}=S_{even}=Ns/2$, whereas E-band states correspond to $|S_{odd}-S_{even}|=1$ and $S_{odd}+S_{even}=(Ns-1)$. These multiplets have $k\neq 0,\ \pi$ and their degeneracy is $N-2$. The actual exchange Hamiltonian is $H_{iso}=H_{rot}+\Delta H$, where ΔH only connects states having the same value of k. Hence L-band and E-band states do not mix in closed homometallic rings. To a very large extent, the effect of ΔH in L-band states is to produce components having $S_{odd}=S_{even}<Ns/2$, i.e., ΔH induces joint quantum fluctuations of the total-spin length of the two sublattices (see Fig. 2). A similar situation of joint fluctuations occurs for E-band states, where the leading corrections have $S_{odd}+S_{even}<(Ns-1)$, but still $|S_{odd}-S_{even}|=1$. The E-band degeneracy $(N-2)$ is partially lifted into $(N-2)/2$ pairs of multiplets, each pair being characterized by a given value of $|k|$.

If the ring is magnetically opened, the rotational bands picture (with $J'=\frac{4(N-1)J}{N^2}$) breaks down (see Fig. 2). In fact, since the shift operator no longer commutes with H_{iso} the wave-vector quantum number is meaningless and only the parity with respect to the remaining in-plane C_2 symmetry can be specified. Of course, this implies that the degeneracy of the k, $-k$ pairs in the E band is removed. The resulting eigenstates therefore contain symmetric and antisymmetric combinations of the previously degenerate k and $-k$ states, called standing-spin waves in Ref. 15. However, the standing-spin-wave component is not the dominant one in most of the actual eigenstates (see Table I). Indeed, states having different values of $|k|$ are strongly mixed. In particular, ΔH directly mixes L-band states ($k=0$ or $k=\pi$) with E-band states having the same S and the same parity. The resulting states contain components with $S_{odd}=S_{even}$ as well as components with $S_{odd}\neq S_{even}$. Hence, in open rings quantum fluctuations of the total spin of the two sublattices do not occur jointly, not even at low temperature. An exception is given by the ground $S=0$ and the ferromagnetic $S=12$ states, which remain very close to those of the closed ring. Indeed, if $S=0$ or $S=12$ there are no E-band states because necessarily $S_{odd}=S_{even}$.

The previous picture can be directly demonstrated by INS experiments. In fact, a mixing of L-band and E-band states has characteristic consequences in the momentum-transfer dependence of the INS intensities, in the effective anisotropy, and in the energy of the lowest-lying $S=1$ states. These aspects will be discussed below, where the labelling of states as

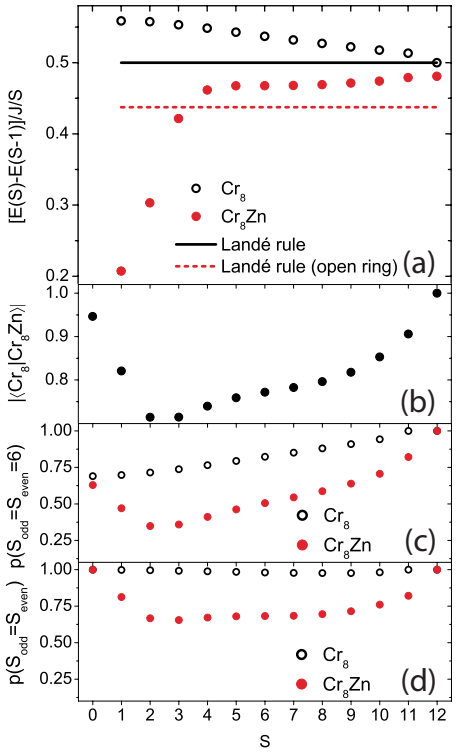

FIG. 2. (Color online) (a) Energy difference between two adjacent levels of the L band for Cr_8 and Cr_8Zn. A deviation from the Landé rule can be seen for the open-ring Cr_8Zn. (b) Modulus of the scalar product between L-band states for the closed Cr_8 and the open Cr_8Zn rings. (c) Weight of the Landé component (i.e., with $S_{odd}=S_{even}=6$) in the L-band states of Cr_8 and Cr_8Zn. (d) Weight of the component with $S_{odd}=S_{even}$ in the L-band states of Cr_8 and Cr_8Zn. This represents the probability of finding the same length for the total-spin of the two sublattices.

L or E is still used for simplicity and refers to the dominant component in the state.

III. INELASTIC NEUTRON SCATTERING EXPERIMENTS

The INS experiments were performed using the time-of flight Disk Chopper Spectrometer at the NIST Center for Neutron Research, Gaithersburg, MD (USA).[16] For the INS experiment, 3.8 g of partially deuterated $[H_2N^{is}Pr_2][Cr_8ZnF_9\{O_2CC(CD_3)_3\}_{18}]$ microcrystalline samples (abbreviated Cr_8Zn-d) have been prepared according to a slightly modified literature procedure reported in Ref. 17 for $[H_2N^{is}Pr^tBu][Cr_8CdF_9\{O_2CC(CH_3)_3\}_{18}]$, by dissolving chromium(III) fluoride trihydrate in a mixture of trimethyl-$d9$-acetic acid and diisopropylamine followed by addition of an excess of the basic zinc carbonate. The preparation of trimethyl-$d9$-acetic acid starting from acetone-$d6$ was adapted from standard methods.[18] Cr_8Zn-d was crystallized from toluene and then dried *in vacuo*. All procedures were performed under dried nitrogen atmosphere and all used solvents were anhydrous. Elemental analysis and the electrospray mass spectrometry confirmed the chemical compositions of this compound. The observed Bragg peaks in x-ray diffraction patterns could be indexed in the monoclinic

TABLE I. Lowest-lying L- and E-like eigenstates of Cr_8Zn (left) in terms of eigenvectors of Cr_8 (right), see also Fig. 3. The states are classified according to their parity with respect to the C_2 symmetry operation (given in the first column). The degenerate $(k,-k)$ E-band states of Cr_8 here have been combined in symmetric and antisymmetric superpositions having definite parity. Only dominant components on L and E states are shown. In Cr_8Zn, several $S=1$ states have a nonzero scalar product with the lowest $S=1$ multiplet of Cr_8, and thus acquire a Landé-type contribution.

	Cr_8Zn	Cr_8
+	$\|L_{S=0}\rangle=$	$0.947\|L_{S=0}\rangle+\cdots$
-	$\|L_{S=1}\rangle=$	$0.821\|L_{S=1}\rangle-0.243\|E^1_{S=1}\rangle-0.242\|E^4_{S=1}\rangle+\cdots$
-	$\|E^1_{S=1}\rangle=$	$0.517\|L_{S=1}\rangle+0.537\|E^1_{S=1}\rangle+0.286\|E^4_{S=1}\rangle+\cdots$
+	$\|E^2_{S=1}\rangle=$	$0.468\|E^2_{S=1}\rangle+0.689\|E^3_{S=1}\rangle-0.318\|E^5_{S=1}\rangle+\cdots$
-	$\|E^3_{S=1}\rangle=$	$0.108\|L_{S=1}\rangle-0.535\|E^1_{S=1}\rangle+0.684\|E^4_{S=1}\rangle+\cdots$
+	$\|E^4_{S=1}\rangle=$	$0.778\|E^2_{S=1}\rangle-0.372\|E^3_{S=1}\rangle+\cdots$
+	$\|E^5_{S=1}\rangle=$	$0.12\|E^2_{S=1}\rangle+0.276\|E^3_{S=1}\rangle+0.843\|E^5_{S=1}\rangle+\cdots$
-	$\|E^6_{S=1}\rangle=$	$0.356\|E^1_{S=1}\rangle-0.77\|E^6_{S=1}\rangle+\cdots$

$P2(1)/c$ space group, with lattice parameters at 100 K of $a=32.2291$ Å, $b=35.7101$ Å, $c=24.1862$ Å, and $\beta=90.544°$. The structure can be described as a nine-membered metallic ring where each Cr···Cr and Cr···Zn edge is bridged by one fluoride and two pivalate ions. The secondary ammonium cation is found encapsulated within the metal wheel.

The sample was packed into a hollow aluminum cylinder (20 mm diameter and 0.7 mm sample thickness) and was inserted into a standard ILL cryostat to cool down to a base temperature of 1.5 K. Measurements were performed at different temperatures, ranging from 1.5 to 15 K. The instrument was operated in the "low-resolution" mode[16] and measurements were performed using four different incident neutron wavelengths, i.e., 3.8, 4.5, 6, and 7 Å. Measurements on an empty Al can were used for the background subtraction and a vanadium sample was used for detector calibration. The spectra were integrated over the whole detector bank. The transition from the $S=0$ ground state to the first $S=1$ excited state in the Landé band was probed with an incident wavelength of 7 Å [42 μeV full width at half maximum (FWHM) energy resolution at the elastic peak]. At a base temperature of 1.5 K we observed two sharp transitions at about 0.2 and 0.3 meV energy transfer [Fig. 4(a)], a much lower energy than what was observed in the Cr_8 parent compound, where the equivalent transitions were observed at 0.7 and 0.9 meV, respectively.[19] Higher energy transitions to the E band could be observed using a lower incident wavelength $\lambda=3.8$ Å (giving a FWHM 230 μeV at the elastic peak), as shown in Fig. 4(b).

The microscopic parameters of the spin Hamiltonian [Eq. (1)] have been varied in order to obtain the best fit of the calculated INS cross section to the neutron data. In the fitting procedure a Gaussian line shape is associated with each allowed transition, with the full width at half maximum fixed to the instrumental resolution and the area proportional to the calculated transition strength. Figure 4 shows the INS spectra collected at $\lambda=7$ Å and $\lambda=3.8$ Å. The solid lines represent

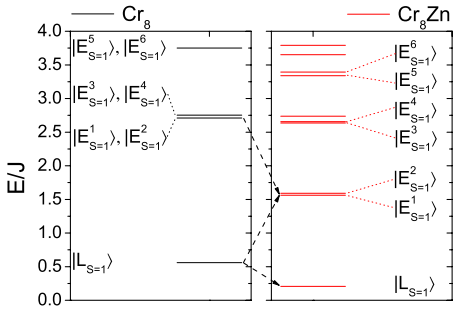

FIG. 3. (Color online) Energy of the low-lying triplet eigenstates of $H_{\rm iso}$ for Cr_8 and Cr_8Zn. For the latter, the labelling of states as L or E refers to the dominant component in the state.

the calculated INS intensity with parameters $J=1.32$ meV, $d=-0.028$ meV, and $|e|=0.003$ meV.[20] In order to improve the fit a small next-nearest-neighbor exchange interaction has to be introduced, with exchange integral $J_{\rm nnn}=-0.01$ meV. Alternatively, a set of slightly bond-dependent nearest-neighbor exchange constants can be assumed. The resulting simulations reproduce the experimental data very well. The uniaxial CF parameter obtained for Cr_8Zn is $d=-0.028$ meV, very close to the one reported for Cr_8 ($d=-0.029$ meV).[19] The two peaks emerging in Fig. 4(a) at 0.2 and 0.3 meV correspond to the transition from the ground-state $|L_{S=0}\rangle$ to the first-excited $|L_{S=1}\rangle$ multiplet, split by the axial anisotropic interactions. The in-plane anisotropy has been taken into account in order to reproduce the correct intensity of the second peak in Fig. 4(a) which involves two otherwise degenerate transitions $|L_{S=0}\rangle \rightarrow |L_{S=1}, M=\pm 1\rangle$.

By reducing the incident wavelength it is possible to observe transitions involving higher-lying excited spin multiplets. In Fig. 4(b), the first peak in the spectrum at $T=1.5$ K originates from the thermally activated transition between the Landé states $|L_{S=1}\rangle$ and $|L_{S=2}\rangle$, while the other peaks are due to transitions from the ground-state $|L_{S=0}\rangle$ to the excited $|E^{1,2}_{S=1}\rangle$ and $|E^{3,4}_{S=1}\rangle$ states. At higher temperatures, two further peaks emerge in the spectrum, corresponding to transitions between the L states $|L_{S=2}\rangle$, $|L_{S=3}\rangle$ and between $|L_{S=1}\rangle$ and the lowest E-type $S=2$ multiplet. We have performed further measurements at intermediate wavelengths that are once again very well reproduced by theoretical simulations.

IV. DISCUSSION

Closed rings are characterized by the presence of a hierarchy of overall INS transition strengths: in decreasing order $L \rightarrow L$ (LL), $L \rightarrow E$ (LE), and $L \rightarrow$ quasicontinuum (LQC). The above-discussed breakdown of the band picture in the open AF ring Cr_8Zn does not unambiguously show up in integrated INS intensities. However, it becomes apparent by inspecting the dependence of the INS intensity $I(Q)$ on the scattering wave vector Q, a quantity which more selectively senses the internal structure of eigenfunctions. The behavior of $I(Q)$ can be understood by expressing the eigenstates of the Cr_8Zn isotropic exchange Hamiltonian in terms of those of Cr_8 (see Table I), and by taking into account that for the

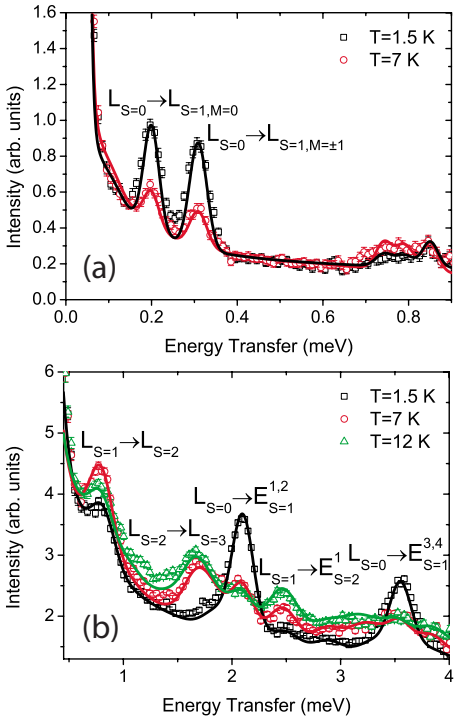

FIG. 4. (Color online) Cr_8Zn INS spectra at low energy collected with $\lambda=7$ Å at $T=1.5$ K (squares) and $T=7$ K (circles) in panel (a) and with $\lambda=3.8$ Å at $T=1.5$ K (squares), $T=7$ K (circles), and $T=12$ K (triangles) in panel (b). Solid lines represent calculated spectra with INS cross section obtained in Ref. 7 and from eigenvalues and eigenvectors of Eq. (1) with the following set of parameters: $J=1.32$ meV, $J_{\rm nnn}=-0.01$ meV, $d=-0.028$ meV, $|e|=0.003$ meV, where $J_{\rm nnn}$ is the parameter of next-nearest-neighbors exchange interaction. The error bars in all the figures represent standard deviations in the measurement.

latter molecule interband INS transitions are less intense than intraband ones. The first-excited $S=1$ state of Cr_8Zn ($|L_{S=1}\rangle$ in Fig. 3) has a dominant contribution from the Landé-band $|L_{S=1}\rangle$ state of Cr_8. Therefore, for the transition between the ground $|L_{S=0}\rangle$ state and $|L_{S=1}\rangle$, $I(Q)$ is similar to that of the corresponding transition of Cr_8 (reported in Refs. 9 and 19). A remarkable difference with respect to Cr_8 is expected for the unresolved transitions between the ground $|L_{S=0}\rangle$ state and states $|E^1_{S=1}\rangle$ and $|E^2_{S=1}\rangle$. In fact, in the open-ring $|E^1_{S=1}\rangle$ acquires a large component of the Landé $|L_{S=1}\rangle$ state of Cr_8. Since a LL transition has much more INS intensity than an LE or an LQC transition, most of the scattering for the unresolved $|L_{S=0}\rangle \rightarrow |E^1_{S=1}\rangle$, $|E^2_{S=1}\rangle$ transitions is produced by the Landé component in $|E^1_{S=1}\rangle$. Thus, $I(Q)$ for these transitions should be close to $I(Q)$ for the $|L_{S=0}\rangle \rightarrow |L_{S=1}\rangle$ transition. This picture is confirmed by the agreement between calculated and experimental $I(Q)$ in Fig. 5(a): the shape of $I(Q)$ is similar for energy transfers around 0.25 and 2 meV. This proves the presence of the Landé-type contribution ($S_{\rm odd}=S_{\rm even}$) to the lowest E state of Cr_8Zn (see Table I). Since all remaining E states contain at most a small fraction of the $|L_{S=1}\rangle$ state of Cr_8, $I(Q)$ for the corresponding $|L_{S=0}\rangle \rightarrow |E_{S=1}\rangle$ transitions is markedly different and recalls that of the $|L_{S=0}\rangle \rightarrow |E_{S=1}\rangle$ transitions of Cr_8 [Fig. 5(b)].

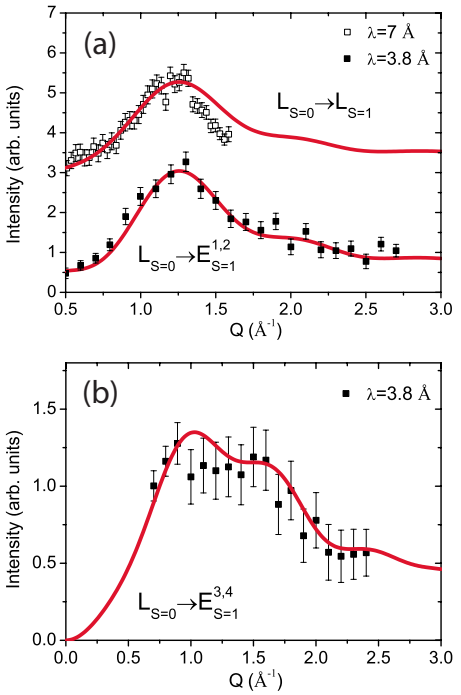

FIG. 5. (Color online) INS spectra as a function of the scattering vector amplitude Q obtained with incident wavelength $\lambda=7$ and 3.8 Å and sample temperature $T=1.5$ K. Calculations are represented by continuous lines. The upper curve and points in panel (a) have been shifted by an offset for clarity.

Another consequence of the breakdown of the band picture is the decrease in the effective axial anisotropy of the $|L_{S=1}\rangle$ multiplet for Cr_8Zn with respect to Cr_8. As we have stressed above, the microscopic axial CF parameter d is almost the same in Cr_8 and Cr_8Zn. However, the way such anisotropy terms project onto the $|L_{S=1}\rangle$ multiplet to split it into a singlet $M=0$ state and a quasidoublet $M=\pm 1$ depends on the internal structure of the multiplet. Indeed, the presence of sizeable E components in the $|L_{S=1}\rangle$ multiplet of Cr_8Zn almost halves its effective anisotropy. The reason is that for the E states of Cr_8, each of the eight local CF terms yields much smaller contributions to the effective anisotropy than for L states of the same S. This effective-anisotropy reduction is directly evidenced by the energy difference between the two peaks at 0.2 and 0.3 meV in Fig. 4(a), which is half the difference observed in Cr_8.[19]

The lowering of the gap between $|L_{S=0}\rangle$ and $|L_{S=1}\rangle$ in Cr_8Zn [Figs. 2(a) and 4(a)] with respect to Cr_8 (Ref. 19) again reflects the presence of E components in $|L_{S=1}\rangle$, i.e., the appearance of disjoint quantum fluctuations of the total spins of the two sublattices. In fact, the ground-state energy in the open ring is nearly $(N-1)/N$ times the ground-state energy of the closed ring as the associated wave functions $|L_{S=0}\rangle$ almost coincide (Table I). On the other hand, $|L_{S=1}\rangle$ in the open ring can be written as $|L_{S=1}\rangle=c_a|a\rangle+c_b|b\rangle$, where $|a\rangle$ and $|b\rangle$ are two orthogonal states characterized respectively by having $S_{\rm odd}=S_{\rm even}$ and $S_{\rm odd}\neq S_{\rm even}$. By considering only the Heisenberg isotropic exchange, the energy $E(L_{S=1})=\langle L_{S=1}|H_{\rm iso}|L_{S=1}\rangle=c_a^2\langle a|H_{\rm iso}|a\rangle+c_b^2\langle b|H_{\rm iso}|b\rangle+c_ac_b[\langle a|H_{\rm iso}|b\rangle+\langle b|H_{\rm iso}|a\rangle]$. For Cr_8Zn the gap is $E(L_{S=1})-E(L_{S=0})\approx 0.21J$ [Figs. 2(a) and 4(a)], much smaller than the gap of $\approx 0.56J$ of Cr_8. The origin of this decrease can be understood by forcing to zero the contribution of the configurations with $S_{\rm odd}\neq S_{\rm even}$, i.e., imposing $c_a=1$ and $c_b=0$. The resulting gap becomes $\approx 0.59J$, even larger than in Cr_8. This shows that the decrease of the gap is not due to a change in the Landé-type ($S_{\rm odd}=S_{\rm even}$) component $|a\rangle$, but rather to the presence of the E-type ($S_{\rm odd}\neq S_{\rm even}$) contributions.

V. CONCLUSIONS

We have performed inelastic neutron-scattering experiments on the magnetically open-ring molecule Cr_8Zn. The set of isotropic exchange and CF interactions parameters necessary to describe the magnetic excitations with energy below about 4 meV have been determined by comparing the experimental cross sections with theoretical predictions. The consequences of the breaking of the ideal ring symmetry have been investigated. The most relevant effect of the ring opening has been found in the structure of eigenstates of the Heisenberg isotropic exchange interaction: the usual classification of low-lying states into distinct rotational bands fails because of the appearance of disjoint quantum fluctuations of the total-spin length of the two sublattices. These fluctuations show up in the measured INS intensity as a function of the scattering wave vector Q, and produce a large decrease in the effective anisotropy with respect to the closed ring. A further consequence is the decrease of the gap between ground- and first-excited multiplets.

ACKNOWLEDGMENTS

We thank M. Bazzani for help in the analysis of INS data. This work utilized facilities supported in part by the National Science Foundation under Agreement No. DMR-0454672.

[1] D. Gatteschi, R. Sessoli, and J. Villain, *Molecular Nanomagnets* (Oxford University Press, Oxford, 2006).
[2] R. Sessoli, D. Gatteschi, A. Caneschi, and M. A. Novak, Nature (London) **365**, 141 (1993).
[3] M. N. Leuenberger and D. Loss, Nature (London) **410**, 789 (2001).
[4] D. Gatteschi, A. Caneschi, L. Pardi, and R. Sessoli, Science **265**, 1054 (1994).
[5] A. Chiolero and D. Loss, Phys. Rev. Lett. **80**, 169 (1998).
[6] F. Troiani, A. Ghirri, M. Affronte, S. Carretta, P. Santini, G. Amoretti, S. Piligkos, G. Timco, and R. E. P. Winpenny, Phys. Rev. Lett. **94**, 207208 (2005).
[7] R. Caciuffo, T. Guidi, G. Amoretti, S. Carretta, E. Liviotti, P. Santini, C. Mondelli, G. Timco, C. A. Muryn, and R. E. P. Win-

penny, Phys. Rev. B **71**, 174407 (2005).
[8] J. Schnack and M. Luban, Phys. Rev. B **63**, 014418 (2000).
[9] O. Waldmann, T. Guidi, S. Carretta, C. Mondelli, and A. L. Dearden, Phys. Rev. Lett. **91**, 237202 (2003).
[10] J. Schnack, M. Luban, and R. Modler, Europhys. Lett. **56**, 863 (2001).
[11] V. O. Garlea, S. E. Nagler, J. L. Zarestky, C. Stassis, D. Vaknin, P. Kögerler, D. F. McMorrow, C. Niedermayer, D. A. Tennant, B. Lake, Y. Qiu, M. Exler, J. Schnack, and M. Luban, Phys. Rev. B **73**, 024414 (2006).
[12] J. Lago, E. Micotti, M. Corti, A. Lascialfari, A. Bianchi, S. Carretta, P. Santini, D. Procissi, S. H. Baek, P. Kögerler, C. Baines, and A. Amato, Phys. Rev. B **76**, 064432 (2007).
[13] A. Ghirri, A. Candini, M. Evangelisti, M. Affronte, S. Carretta, P. Santini, G. Amoretti, R. S. G. Davies, G. Timco, and R. E. P. Winpenny, Phys. Rev. B **76**, 214405 (2007).
[14] Y. Furukawa, K. Kiuchi, K.-i. Kumagai, Y. Ajiro, Y. Narumi, M. Iwaki, K. Kindo, A. Bianchi, S. Carretta, G. A. Timco, and R. E. P. Winpenny, Phys. Rev. B **78**, 092402 (2008).
[15] S. T. Ochsenbein, O. Waldmann, A. Sieber, G. Carver, R. Bircher, H. U. Güdel, R. S. G. Davies, G. A. Timco, R. E. P. Winpenny, H. Mutka, and F. Fernandez-Alonso, Europhys. Lett. **79**, 17003 (2007).
[16] J. R. D. Copley and J. C. Cook, Chem. Phys. **292**, 477 (2003).
[17] G. A. Timco, A. S. Batsanov, F. K. Larsen, C. A. Muryn, J. Overgaard, S. J. Teat, and R. E. P. Winpenny, Chem. Commun. (Cambridge) **2005**, 3649.
[18] B. S. Furniss, A. J. Hannaford, P. W. G. Smith, and A. R. Tatchell, *Vogel's Textbook of Practical Organic Chemistry*, 5th ed. (Longman, New York, 1989).
[19] S. Carretta, J. van Slageren, T. Guidi, E. Liviotti, C. Mondelli, D. Rovai, A. Cornia, A. L. Dearden, F. Carsughi, M. Affronte, C. D. Frost, R. E. P. Winpenny, D. Gatteschi, G. Amoretti, and R. Caciuffo, Phys. Rev. B **67**, 094405 (2003).
[20] The axial dipole-dipole interaction and the single-ion axial anisotropies have similar effects. Therefore, a very good agreement between calculated and measured INS spectra is obtained also if the d parameter is rescaled to the value of $d=-0.036$ meV, and understood as to include both the CF and the dipolar contributions.